



Earth, Environmental and Life Sciences

Princetonlaan 6
3584 CB Utrecht
P.O. Box 80015
3508 TA Utrecht
The Netherlands

www.tno.nl

T +31 88 866 42 56

infodesk@tno.nl

TNO report

TNO-060-UT-2012-00508

Two-way coupling of RACMO2 and LOTOS-EUROS

Implementation of the direct effect of aerosol on radiation

Date	19 April 2012
Author(s)	Drs. M. (Mark) Savenije, KNMI Dr. L.H. (Bert) van Uft, KNMI Dr. E. (Erik) van Meijgaard, KNMI Dr. J.S. (Bas) Henzing, TNO J.M.J. (Joost) Aan de Brugh MSc, TNO Dr. A.M.M. (Astrid) Manders-Groot, TNO Dr. M. (Martijn) Schaap TNO
Number of pages	35
Number of appendices	-
Sponsor	NMDC
Project name	Lukwa en Externe Veiligheid
Project number	034.23884

All rights reserved.

No part of this publication may be reproduced and/or published by print, photoprint, microfilm or any other means without the previous written consent of TNO.

In case this report was drafted on instructions, the rights and obligations of contracting parties are subject to either the General Terms and Conditions for commissions to TNO, or the relevant agreement concluded between the contracting parties. Submitting the report for inspection to parties who have a direct interest is permitted.

© 2012 TNO

Contents

1	Introduction	4
2	Implementation of the aerosol direct effect	7
2.1	Baseline: Tegen climatology.....	7
2.2	Implementation of LOTOS-EUROS aerosols in RACMO2.....	9
3	Experiments	17
4	Results	19
4.1	Yearly mean patterns.....	19
4.2	Comparison to AERONET observations	25
5	Discussion.....	29
6	References	31
7	Signature	35

1 Introduction

Atmospheric aerosol, or particulate matter (PM), has an adverse impact on the health of human beings and other organisms. There are strict regulations for concentrations (e.g. EU (2008), US EPA NAAQS) and the quantification of expected changes in concentrations is therefore highly relevant for policy making. Aerosol also plays an important role in the climate system by its interaction with radiation (absorption and scattering) and/or cloud formation and cloud properties (IPCC 4th assessment report and references therein). The day-to-day and even sub-daily variability of concentrations strongly depends on atmospheric conditions, since these govern transport, dilution and deposition, as well as chemical conversions (cloud processes, photochemistry). The correlation of particulate matter with meteorological parameters is complex and depends on the component (e.g. Tai et al. 2010, Jimenez-Guerrero et al 2011, Manders et al 2011, Mues et al, 2012). Due to changes in meteorology related to a changing climate, ambient concentrations are expected to change even if anthropogenic emissions are kept constant. Therefore, further emission reductions may be needed to comply with regulations under expected warmer conditions. Moreover, changes in aerosol concentrations may lead to changes in surface temperature or alter the characteristics of clouds and precipitation (Raes et al. 2010). These feedback mechanisms can presently be taken into account in coupled weather and atmospheric chemistry models (Zhang et al 2010), although most models can only perform short simulations due to the high computational costs.

The regional chemistry transport model LOTOS-EUROS (Schaap et al. 2008) has been coupled to the regional climate model RACMO2 (Lenderink et al 2003, Van Meijgaard et al 2008). In contrast to most existing coupled systems, the model system RACMO-LOTOS-EUROS offers the feasibility of performing long-term simulations with an acceptable throughput time. A one-way coupled version of the system, which uses meteorological fields from RACMO2 to drive LOTOS-EUROS, was used to generate long-term simulations (1970-2060) to study the impact of climate change on air quality (Manders et al 2011, Manders et al 2012). In contribution to the Climate change Spatial Planning (CcSP) programme a two-way coupled system was developed with the aim to quantify the role of the first aerosol indirect effect (AIE, effect of particles on cloud condensation) in climate change on the regional scale. In this framework, aerosol mass information from LOTOS-EUROS (sulfate, nitrate, sea salt) is fed back to RACMO2 and, utilizing a parametric formulation proposed by Menon et al. (2002), converted into number concentrations of cloud condensation nuclei (De Martino et al 2008). These number concentrations are subsequently combined with the RACMO2 simulated liquid water contents to determine the corresponding effective radius. In the model formulations this is the primary parameter in controlling the interaction between clouds and solar radiation. Results obtained with the uncoupled RACMO have been used as a reference. In the uncoupled version the effective radius is determined with the empirical diagnostic formulation by Martin et al. (1994). Comparison of present-day climate integrations (1971-2000) with the two-way coupled and the uncoupled system showed a discernable impact of the first AIE to the amount of global radiation and, to a lesser extent, near surface temperature (<1K) in Northern and Central Europe. However, assuming a constant aerosol emission scenario the climate change effect of the first AIE (difference between 2031-2060 and 1971-

2000) was found negligible suggesting that model clouds appear remarkably unaffected in a future warming climate.

The present report describes the extension of RACMO2-LOTOS-EUROS with an explicit treatment of the aerosol direct effect: the impact of aerosol on radiation through scattering and absorption by aerosol. The extension is meant to replace the existing implementation of the aerosol direct effect in RACMO2 which was adopted from ECMWF IFS Cycle 31 some years ago. That approach was based on combining prescribed fixed spatial patterns of various aerosol species with their associated effective aerosol optical parameters according to the Tegen climatology (Tegen et al., 1997). The Tegen climatology contains a seasonal cycle, includes spectral optical properties, contains a vertical structure depending on the combination of the seven included aerosol classes, and contains volcanic and stratospheric aerosol. However, because it is a climatology, temporal and spatial variations in aerosol optical properties are not captured. A significant improvement is expected when space-time varying aerosol loadings are used. LOTOS-EUROS has a long tradition in aerosol modeling. It is used for daily operational smog forecasting in the Netherlands (Manders et al 2009, De Ruijter de Wildt et al. 2011) and has participated in several European model intercomparison studies and scenario studies (EURODELTA).

The technical part of the coupling (scripts, interpolations, conventions) is described in a separate report (Savenije et al 2012). The present report describes the scientific approach. In Section 2, first the aerosol climatology by Tegen is described, then the method to include LOTOS-EUROS aerosol fields is introduced schematically. After that, each of the steps is discussed in more detail. In section 3 model simulations are described and the results are presented in section 4.. They are compared with observations from AERONET. Finally, the results are discussed and points for improvement and follow-up are outlined.

2 Implementation of the aerosol direct effect

2.1 Baseline: Tegen climatology

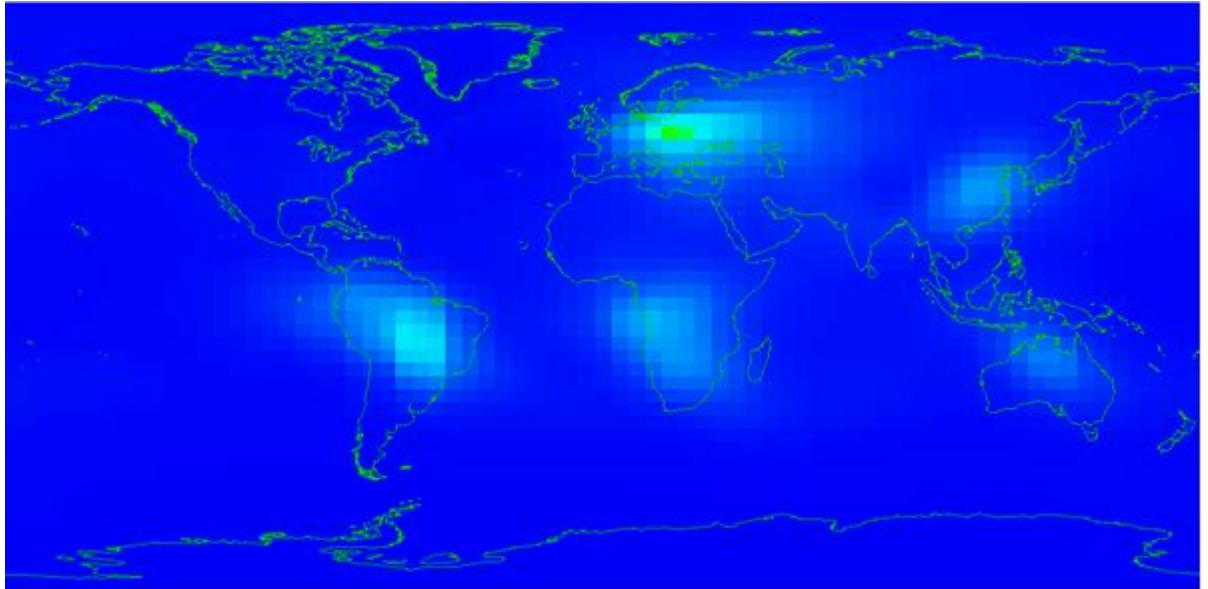


Figure 1 Tegen climatology for black carbon in August

The Tegen aerosol climatology (Tegen et al., 1997) exhibits a spatial structure which is similar to the Tanré climatology (Tanré et al., 1985) used in earlier cycles of the ECMWF IFS, but is temporally somewhat more extended as it contains a seasonal cycle. Also, aerosol optical parameters are wave-length dependent. Finally, the vertical structure of the aerosol is generated by an aerosol class dependent (but otherwise fixed) profile, where the (columnar) aerosol optical depth (AOD) serves as the basis.

In the Tegen aerosol climatology six aerosol types are considered: organic, sulphate, sea salt, dust-like or soil-dust, and black carbon. The basic input consists of space-time varying maps of these aerosols expressed as aerosol optical depths determined at $0.55\mu\text{m}$ (or 550nm). The spatial variation is expressed on a $5^\circ \times 4^\circ$ geographic lon-lat grid ($n_{\text{lon}} = 72$; $n_{\text{lat}} = 46$). The climatology contains seasonal variation (12 month values), but no interannual variation. The optical depths are established with fixed (aerosol dependent) relative humidities.

An example of the August climatology of black carbon is displayed in Figure 1. It shows a significant maximum in climatological amount of black carbon over Eastern Europe and West-Russia (related to traffic and industry), while less prominent black carbon spots are seen over Brazil and the region of Angola (related to bio mass burning). It should be noted that the Tegen et al. climatology is compiled primarily on the basis of data collected in the eighties and early nineties of the 20th century.

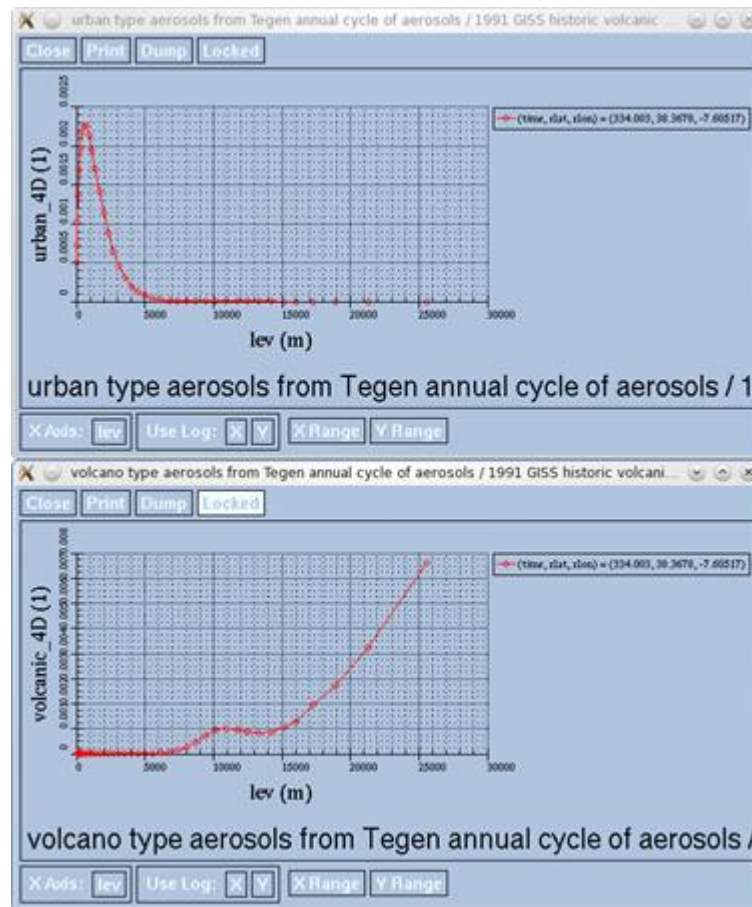


Figure 2 Height distribution function of AOD for urban and volcano type aerosol

In addition, a GISS history of volcanic aerosol is prescribed for the period 1957-2010, including both monthly and interannual variations, in terms of zonally averaged amounts on a 24-point latitude grid (7.8° resolved). This distribution is mapped on the same 46-point latitude mesh used for the Tegen aerosols. For each aerosol class and in each spectral interval (6 bands in the old short wave scheme; 14 bands in the new short wave SRTM code) the following aerosol optical parameters are specified: optical thickness, single scattering albedo, asymmetry factor.

Figure 2 shows typical “idealized” fixed vertical profiles for two aerosol classes, i.e. the urban type aerosol, confined the atmospheric boundary layer and lower troposphere, and the volcano type aerosol, located in the upper troposphere and stratosphere. Figure 3 shows the GISS climatology used in the ECMWF IFS for the period 1957-2010. The marked peaks correspond to the major volcanic eruptions in the past half century: Mount Pinatubo, Philippines, 1991; El Chichón, Mexico, 1982; Mount Agung, Indonesia, 1963.

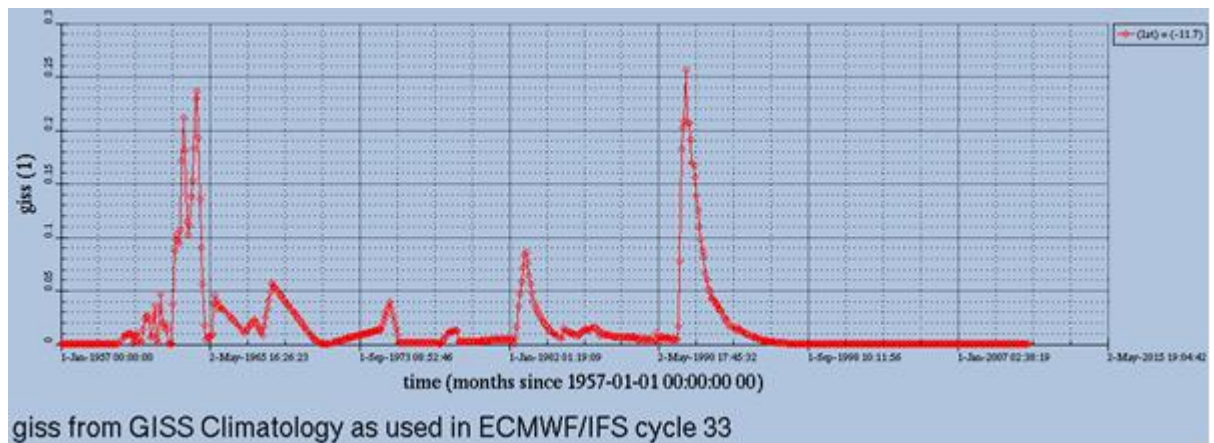


Figure 3 AOD of GISS climatology zonally averaged along 11.7° S

2.2 Implementation of LOTOS-EUROS aerosols in RACMO2

Replacing the Tegen climatology by space-time varying aerosol fields from LOTOS-EUROS (LE) is expected to yield more realistic radiation fields. The effect of aerosol on radiant energy is incorporated in RACMO2 by specifying (aerosol) optical depth, single scattering albedo, and asymmetry parameter for the 14 spectral intervals that are used in the new RRTM-SW radiation scheme (Mlawer and Clough, 1997), which was recently adopted in RACMO2 from ECMWF Cycle 33r1. Hereafter, the new short wave radiation scheme is referred to as SRTM. The implementation requires the LOTOS-EUROS mass concentrations to be translated into these three parameters on the RACMO grid. To do so, a number of consecutive conversion steps needs to be performed. These steps are:

1. Conversion from LE to RACMO2 grid
2. Assigning mass to aerosol modes
3. Calculate water uptake
4. Convert aerosol mass to volume
5. Calculate aerosol number concentration
6. Calculate refractive indices from lookup tables
7. Extract optical parameters from lookup tables
8. Combine and finalize calculations

In the first step (1) the LOTOS-EUROS fields are remapped to RACMO grid in both horizontal and vertical directions. Then (step 2) aerosol mass concentrations of nine aerosol tracers are assigned to two distinct modes. Within these modes, the contributing species are assumed to be internally mixed and the mass is assumed to be log-normally distributed. The first mode is hereafter referred to as accumulation mode, the second mode is referred to as coarse mode. LE modeled aerosol is dry, but in reality aerosols contain water.

This aerosol-water impacts on the optical properties and should therefore be considered (step 3). The amount of water depends on the size (Kelvin effect), aerosol chemistry (solute effect or Raoult effect), and the availability of water vapor. For the optically active particles considered in this study, the Kelvin effect can safely be neglected. The growth of an aerosol particle due to water uptake can then be described by a simple hygroscopic growth factor that depends on the relative humidity and a specie dependent coefficient that is a measure of the particle's hygroscopicity. For internal mixtures of chemical components, that comprise the modes in this study, a simple volume weighted mixing rule can be applied to obtain the appropriate coefficient representative for the mode. For the three optical parameters that are finally to be obtained Look-Up-Tables (LUT) are made. In the LUTs optical properties for a single particle are given for a range of refractive indices and optical wavelengths that encompasses the range of atmospheric aerosol and spectral intervals of interest. Consequently, the number of particles that build up the given dry mass in the modes must be deduced. The next step is therefore to deduce the aerosol volume in the modes (step 4) and to convert the median diameter, which describes the mode, into a volume mean diameter so that the number of particles in the modes can be obtained (step 5). For typical atmospheric aerosol, composite refractive indices are rather insensitive to the choice of mixing rule and hence a simple volume-weighted average of individual refractive indices of the species that comprise the internal mixtures in the two modes, can be used (Lesins et al., 2002) to calculate effective refractive indices (step 6). For the effective refractive indices and humidified aerosol size the optical parameters can now be subtracted from the LUT (step 7). For the optical depth, the contribution of both modes can be summed for each of the 14 spectral intervals. For the single scattering albedo, the effective value can be obtained by the ratio of total scattering over total extinction. For the asymmetry parameter the contribution from both modes is accounted for by weighing the two asymmetry parameters with the fractional contribution to the total scattering.

These steps will now be discussed in more detail.

Ad 1 Conversion from LE to RACMO2 grid

For the translation of the RACMO2 grid (rotate pole grid) to the LOTOS-EUROS grid (10° W-40° E, 35-70° N, 0.5×0.25° lon×lat resolution, 5 km in vertical with 4 dynamical vertical layers + surface layer) we refer to the NMDC technical Coupling report (Savenije et al 2012). Since the RACMO2 domain is encompassing the LOTOS-EUROS domain, the Tegen climatology is used in RACMO2 in the small areas outside the LOTOS-EUROS domain and above 5 km. Since LOTOS-EUROS version 1.6 does not give reliable dust output, also for dust the Tegen climatology is used in RACMO2,. The most recent LOTOS-EUROS version (v1.8) does contain realistic dust fields which can in principle be used without further adaptations to the coupling and parameterizations.

Ad 2 Distinguish fine and coarse mode species

LOTOS-EUROS outputs dry aerosol mass concentrations. The aerosol mass is already partitioned into two distinct modes, i.e. fine and coarse mode, and this classification is static. In Table 1 the modes are listed. The fine mode is hereafter referred to as mode 1 or as accumulation mode. The coarse mode is referred to as mode 2 or coarse mode. The particles in each mode are assumed to be log-normally distributed and their distribution is characterized by a median diameter D_{pg} and a geometric standard deviation σ_g .

The median diameter is the diameter separating the 50% smallest particles from the 50% largest particles. The geometric standard deviation is a measure of the width of the log-normal distribution, i.e. 67% of all particles lies in the range from D_{pg}/σ_g to $D_{pg}\times\sigma_g$, e.g. $\sigma_g = 1$ is a monodisperse distribution. Remark: Although dust is listed as a LOTOS-EUROS field, it stems from the climatology of Tegen et. Al. (1997) in this study.

Specie	Specie mode 1=accumulation 2=coarse	Hygroscopic coefficient K (Petters and Kreidenweis 2007)	Density (g/cm ³)	LOTOS-EUROS field in conc-3d output file
Black carbon	1	0.0	1.0	Bcar
Organics	1	0.1	1.9	Ppm25
Sea salt Fine	1	1.0	2.165	Na_f
Sea salt Coarse	2	1.0	2.165	Na_c
Sulfate	1	0.5	1.77	Sulf
Ammonium	1	0.7	1.7	Ammo
Nitrate	1	0.7	1.5	Nitr
Dust Fine	1	0.0	2.65	Dust_f
Dust Coarse	2	0.0	2.65	Dust_c

Table 1 Specie properties

Ad 3 Calculate water uptake

The growth of aerosols due to water uptake is described by the hygroscopic growth factor $g(RH)$. The $g(RH)$ is defined as the particle diameter in equilibrium with its ambient relative humidity $D_{wet}(RH)$ divided by its dry diameter D_{dry} :

$$g(RH) = \frac{D_{wet}(RH)}{D_{dry}} \quad 1$$

The one-parameter approximation of $g(RH)$ that is used to calculate the growth for each grid cell is proposed by Petters and Kreidenweis (2007):

$$g(RH) = \left(1 + \kappa \frac{RH}{1 - RH} \right)^{\frac{1}{3}}, \quad 2$$

where the coefficient κ is a measure of the particle's hygroscopicity.

For a complex internal mixture of chemical components, the value of the coefficient κ is given by the simple mixing rule:

$$\kappa_i = \sum_{n_i} \varepsilon_{n_i} \kappa_n, \quad 3$$

where the subscripts n and i refer to the species comprising the mixture and the particle mode, respectively, while ε_n is the volume fraction occupied by specie n : thus ε_n is ratio of the dry volume of specie n and the volume of all species (excluding water) in the specific mode (estimates provided in section 3). The one-parameter approximation of the growth function $g(\text{RH})$ that is implemented in RACMO2 yields results that comply with e.g. the growth function that is used within LOTOS-EUROS (Figure 4).

Remark: In the current implementation the relative humidity is cut off at 95%.

Ad 4 Convert aerosol mass to volume

With use of the densities supplied in the Table 1 it is straightforward to obtain the volumes occupied by the aerosols, assuming spherical particles.

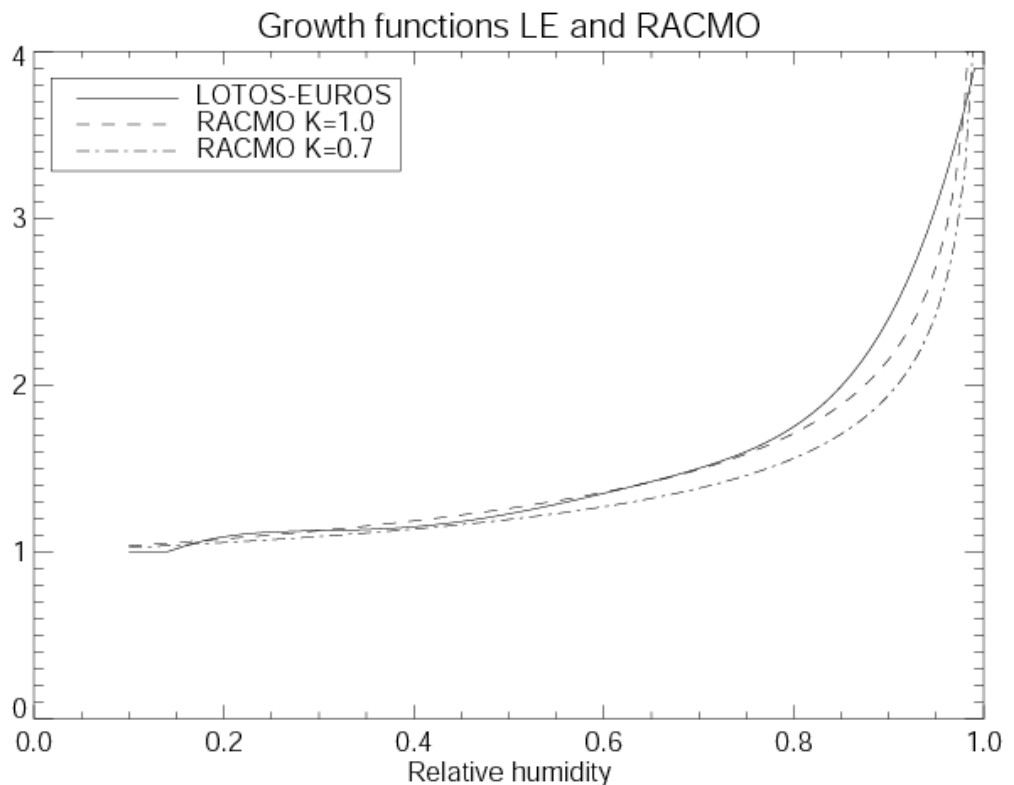


Figure 4 RACMO2 and LOTOS-EUROS growth functions

Ad 5 Calculate aerosol number concentration

A recent article by Asmi et al. (2011) presents harmonized aerosol distribution data from 24 European field monitoring sites over 2008-2009. Though there are spatial and temporal variations, attention has been given to the usability of the results for aerosol modeling purposes.

From these data uniform fitting parameters for modeling the LOTOS-EUROS mass concentrations into aerosol number concentrations have been extracted: For fine mode a geometric mean diameter of 159 nm is used with a geometric standard deviation of 1.59. Coarse mode parameters have been set on 2 μm and 2.0. Initial calculations showed however that fine mode AODs turned out to be rather low. In most of the validation runs another setting for the fine mode lognormal fit parameters is used for comparison: alternative values used are 300 nm and 1.35, which yield intermediate values for the AOD. In Figure 5 the sensitivity in (columnar) optical depth (AOD) to the use of different fine-mode parameters is illustrated for a sample of sulfate aerosol with concentration $10\mu\text{g}/\text{m}^3$. The Figure clearly shows that application of the alternative values in specifying the geometric mean diameter and standard deviation leads to higher values in AOD for the entire wave length spectrum beyond 350 nm.

In the LUT the optical properties for a single particle are given. The modeled quantity is mass. Thus it is necessary to deduce the number of particles that built up the given dry mass (volume). Note: aerosol humidity growth affects the size of particles but not their number concentration.

At this point we need to be more specific about the assumed modes. For the accumulation mode the dry median diameter $D_{pg} = 700\text{nm}$ and the geometric standard deviation $\sigma_g = 1.59$. For the coarse mode $D_{pg} = 4\mu\text{m}$ and $\sigma_g = 2.0$.

To deduce the particle number concentration, two relations are important (e.g. Seinfeld and Pandis 2006):

1) If the number distribution is lognormal, the volume distribution is also lognormal with the same geometric standard deviation and the volume median diameter D_{pgv} is given by:

$$\ln D_{pgv} = \ln D_{pg} + 3 \ln^2 \sigma_g \quad \text{thus:} \quad 4$$

$$D_{pgv} = \exp(\ln D_{pg} + 3 \ln^2 \sigma_g) \quad 5$$

2) For a lognormal distribution the relation between the mean diameter D_p and the median diameter is given by:

$$D_p = D_{pg} \exp\left(\frac{\ln^2 \sigma_g}{2}\right) \quad \text{and likewise:} \quad 6$$

$$D_v = D_{pgv} \exp\left(\frac{\ln^2 \sigma_g}{2}\right) \quad 7$$

Conversion to volume mean diameter D_v is convenient since all particles having size D_v would give the same volume as is obtained when integrating the full size distribution. The total number concentration in mode i can thus be written:

$$N_T^i = \frac{V_T^i}{\left(\frac{1}{6} \pi (D_v^i)^3\right)} \quad 8$$

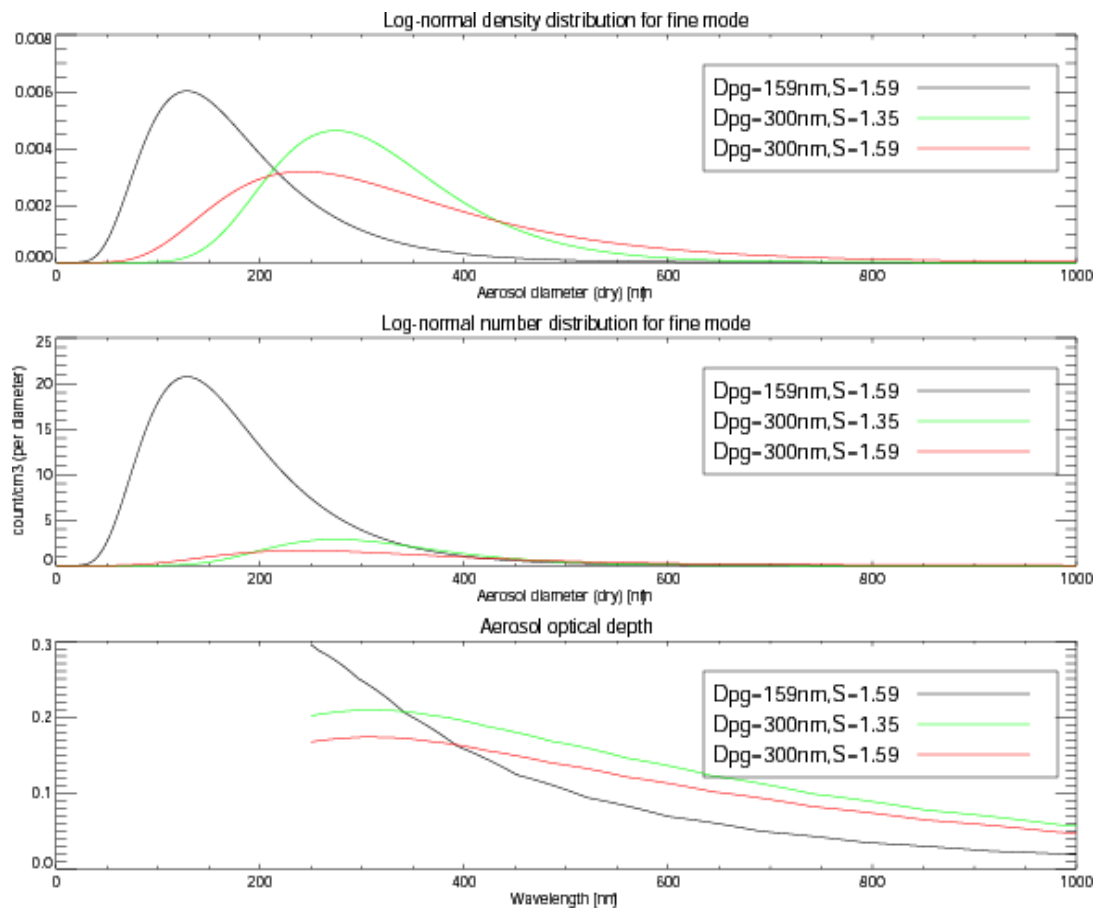


Figure 5 Difference in density and number distribution, and in AOD for a fine mode sulfate aerosol sample assuming different parameters in specifying the lognormal distributions. The grey line refers to the standard settings, the green line to an alternative setting, while the red line represents a hybrid choice

Ad 6 Calculate refractive indices

As discussed hereafter the refractive indices for the composite aerosols are approximated by the relative weight of the individual aerosols in these composite aerosols. The refractive indices of the components are extracted from a lookup table (LUT) that are specific for an aerosol. Several databases are used: the OPAC database (Hess et al., 1998) is used for sulphate, black carbon and sea salt. ECHAM-HAM (Kinne et al., 2003) supplies values for particulate matter and dust and the Segelstein (1981) table contains the refractive index for water. All databases consist of values for a number of wavelengths and the values for the specific RACMO2 spectral bands are obtained by means of interpolation.

For typical atmospheric aerosol, composite refractive indices are rather insensitive to the choice of mixing rule and hence a simple volume-weighted average of individual refractive indices can be used (Lesins et al., 2002). Important input here are the refractive indices of the 9 LE-species for the 14 wavelength bands used in the optical model.

For n =species (1,9), i =modes (1,2), j =wavelengths (1-14) and Re is real part refractive index, and Im is imaginary part refractive index:

The real and imaginary part of the refractive index for each mode ($i=1-2$) and spectral interval ($j=1-14$) are obtained by summing over the aerosol specie ($n=1-9$)

specific real and imaginary part of the refractive index weighted over the mode and specie specific (wet) volume,

$$\text{Re}_j^i = \frac{\sum_n V_n^i \cdot \text{Re}_n^j}{V_T^i} \quad \text{and} \quad 9$$

$$\text{Im}_j^i = \frac{\sum_n V_n^i \cdot \text{Im}_n^j}{V_T^i}, \quad 10$$

where V_n^i denotes the volume of the wetted specie n and mode i

Ad 7 Extract optical parameters from lookup tables

Now the refractive indices and the (wetted) aerosol size are known, the optical parameters (cross section, single scattering albedo (SSA) and asymmetry factor (ASYM)) can be found by means of another set of six lookup tables (two modes times three optical parameters). These tables have been created to avoid intense calculations during model execution. They are built around the two geometric standard deviations of 1.59 and 2.0 for the fine and coarse mode, respectively, and consist of 60.000 values for ranges of the refractive indices and aerosol size. Finally, taking the results for the fine and coarse mode together yields all aerosol related parameters required in the radiation code.

Aerosol optical depth

To obtain the model grid-cell aerosol optical depth (AOD) for a specific spectral band (wavelength λ):

- extract the dimensionless extinction cross sections (f_1^i) from the first set of lookup-tables for both modes i .
- Multiply f_1^i with the square of the chosen specific wavelength, to get the extinction cross section normalized to a single particle (σ_{ext}^i)

$$\sigma_{ext}^i = f_1^{\text{mode-1}} \cdot (\lambda_j)^2$$
- Multiply σ_{ext}^i with the total number concentration of particles in the grid cell ($N_T^i/\text{volume grid-cell}$), to obtain the extinction coefficient (k_{ext}^i [m^{-1}])

$$k_{ext}^i = f_1^{\text{mode-1}} \cdot (\lambda_j)^2 \cdot N_T^{\text{mode-1}}$$
- Sum the extinction coefficients from both modes and multiply with the geometrical grid cell thickness Δz to finally obtain the AOD.
- Note: the λ -dependence of f_1^i , σ_{ext}^i , and k_{ext}^i , are here omitted for simplicity.

In formulas:

$$\text{AOD}(\lambda_j) = \left(f_1^{\text{mode-1}} \cdot (\lambda_j)^2 \cdot (N_T^{\text{mode-1}}) + f_1^{\text{mode-2}} \cdot (\lambda_j)^2 \cdot (N_T^{\text{mode-2}}) \right) \Delta z \quad 11$$

The index j denotes each of the 14 spectral bands, here represented by a single central wavelength, in the optical module.

Single scattering albedo

In order to obtain the single scattering albedo (SSA) the outcome of the two modes cannot be straightforwardly added as for AOD, however it turns out that the SSA of a complex single particle is equal to the ensemble of particles that builds up the aerosol population. This means that only SSA^1 and SSA^2 extracted from the LUTs

for modes 1 and 2, respectively, need to be combined. SSA is defined as the ratio of the scattering coefficient and the extinction coefficient, where the extinction coefficient (k_{ext}^i) is the sum of the absorption coefficient (k_{abs}^i) and the scattering coefficient (k_{sca}^i). The extinction coefficient is one of the products obtained as an intermediate step in constructing the AOD, therefore:

$$k_{sca}^i = k_{ext}^i \cdot SSA^i \quad 12$$

$$SSA_{total}(\lambda_j) = \frac{k_{sca}^1 + k_{sca}^2}{k_{ext}^1 + k_{ext}^2} \quad 13$$

Asymmetry parameter

The asymmetry parameters (ASYN) of both modes are combined by weighing the g-factors of both modes with the respective mode-specific fractional contribution to the total scattering:

$$g_{Total}(\lambda_j) = \frac{k_{sca}^1 \cdot g^1 + k_{sca}^2 \cdot g^2}{k_{sca}^1 + k_{sca}^2} \quad 14$$

3 Experiments

To test the new aerosol direct effect component of the coupled system and to explore its impact on climate parameters we have conducted a number of short-term experiments at the ECMWF computing systems. All experiments are carried out with the default settings for a coupled run: RLOTOS50 domain, time step of 15 minutes and the exchange between the two models done every three hours. 32 cores are used for both RACMO2 as LOTOS-EUROS. Using more cores in order to speed up the integration is not possible due the OpenMP setup of LOTOS-EUROS. On the current ECMWF computer the coupled run proceeds by one model year every 36 hours. Most results that are presented are derived from three experiments. All three experiments run from May 2007 until May 2009. The first year is used as spin-up and allows sufficiently time for temperatures to adapt. All analysis is done for one full year: May 2008 until May 2009 (which happens to be the observation period of the EUCAARI project (European Integrated project on Aerosol Cloud Climate and Air Quality Interactions)).

The first experiment serves as a control run and utilises the Tegen aerosol climatology (this run is addressed as the reference run). The two other experiments incorporate the LOTOS-EUROS aerosol driven implementation of the direct aerosol effect. We conducted two experiments with different aerosol size distributions for the fine mode: The first with an aerosol diameter of 159nm and a geometric standard deviation of 1.59, the second with a diameter of 300nm and a standard deviation of 1.35. Motivation for the experiment with increased diameters came from the consideration that the calculated AOD's seemed rather low at first look and increasing diameter size greatly influences the AOD as was discussed before in Figure 5 (shown by the grey and green curve, respectively).

4 Results

4.1 Yearly mean patterns

In Figure 6 the yearly mean AOD is shown. The left panels of the Figure contain, from top to bottom the AOD for the reference run, the 159/1.59 aerosol size distribution (LE_159) and 300/1.35 (LE_300) distribution. On the right side the difference with respect to the reference run is depicted. Easily recognizable is the interior domain which is loaded with the LOTOS-EUROS aerosols where AOD values are significantly lower than according to the Tegen climatology. In particular for the LE_159 experiment annual mean AOD values are 0.10 up to 0.3 smaller over the European land mass (with the exception of Spain and Scandinavia) compared to Tegen, which is more than 50% in a relative sense. But also for the LE_300 experiment the AOD is found to be lower than for the Tegen estimate almost everywhere. This result strongly suggests that the Tegen et al. climatology does not provide an adequate AOD value for present-day climate conditions across continental Europe.

In this respect, a better reference may be inferred from the aerosol forcings compiled in the framework of CMIP5 which were very recently made available in the uncoupled version of RACMO. Figure 7 compares the AOD-values derived from LOTOS-EUROS, from the CMIP5 aerosol forcing, and from the Tegen climatology. The figure shows that LOTOS-EUROS and CMIP5 are much closer to each other than LOTOS-EUROS and Tegen. In upcoming experiments, we will therefore adopt the CMIP5 aerosol forcings to serve as the reference.

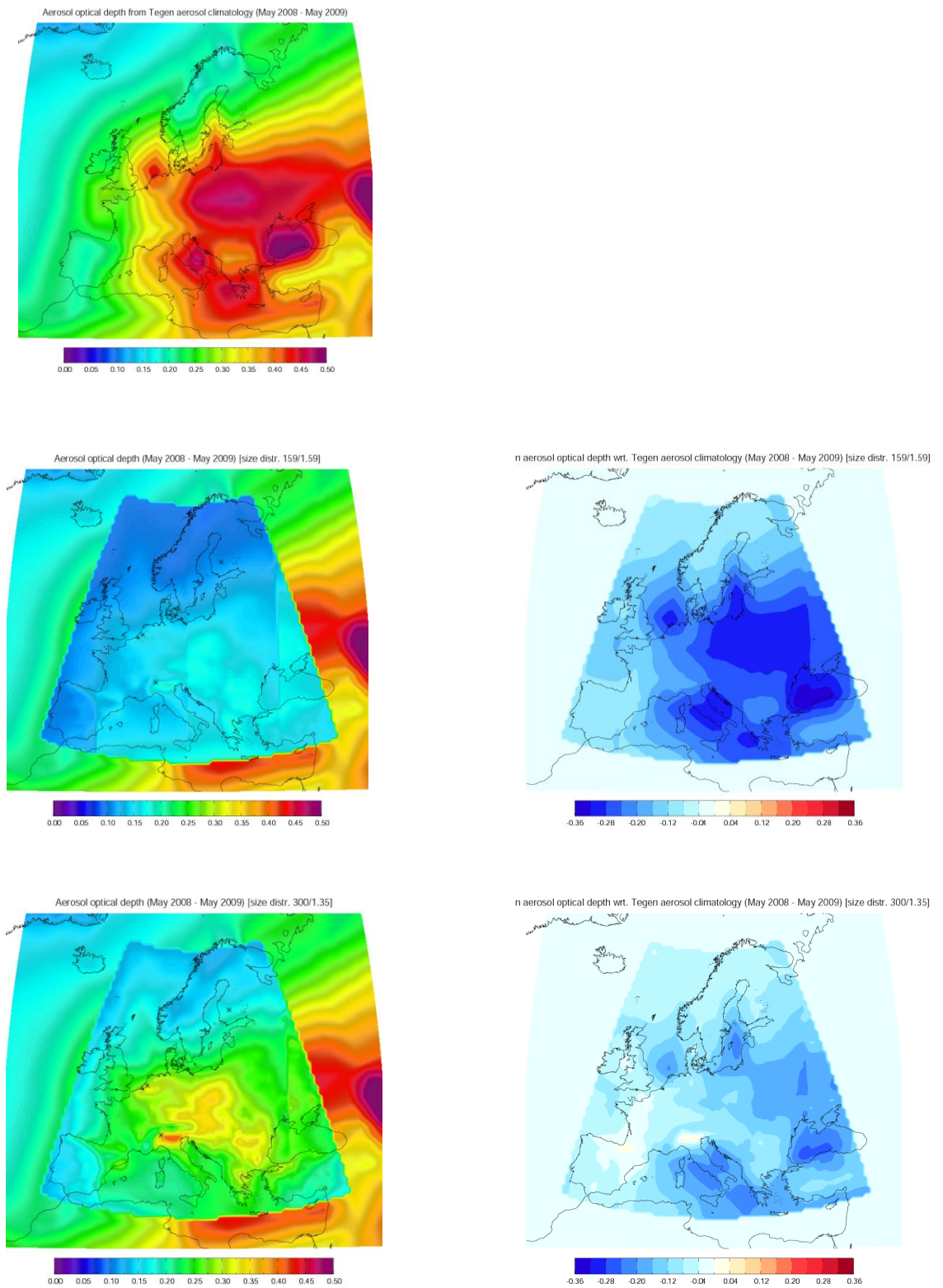


Figure 6 Yearly mean AOD for the Tegen climatology (top left panel), the 159/1.59 aerosol size distribution (central left panel), and the 300/1.35 distribution (bottom left panel). The plots on the right hand side depict the difference with respect to the reference

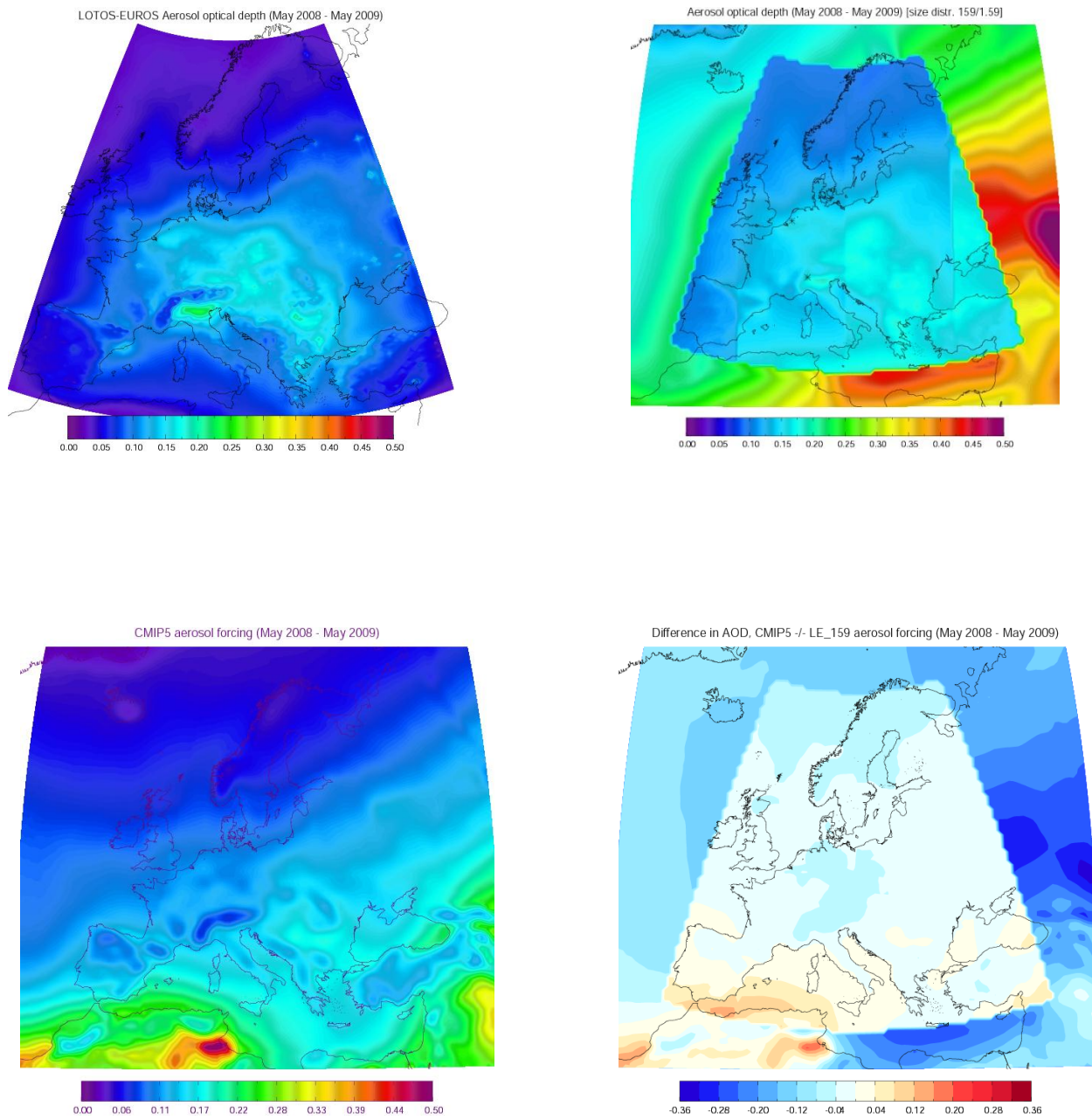


Figure 7 Top left shows the yearly mean AOD as calculated directly by LOTOS-EUROS. Top right shows the new AOD from LE_159. Bottom row shows the AOD inferred from CMIP5 aerosol forcings; mean and difference to LE_159

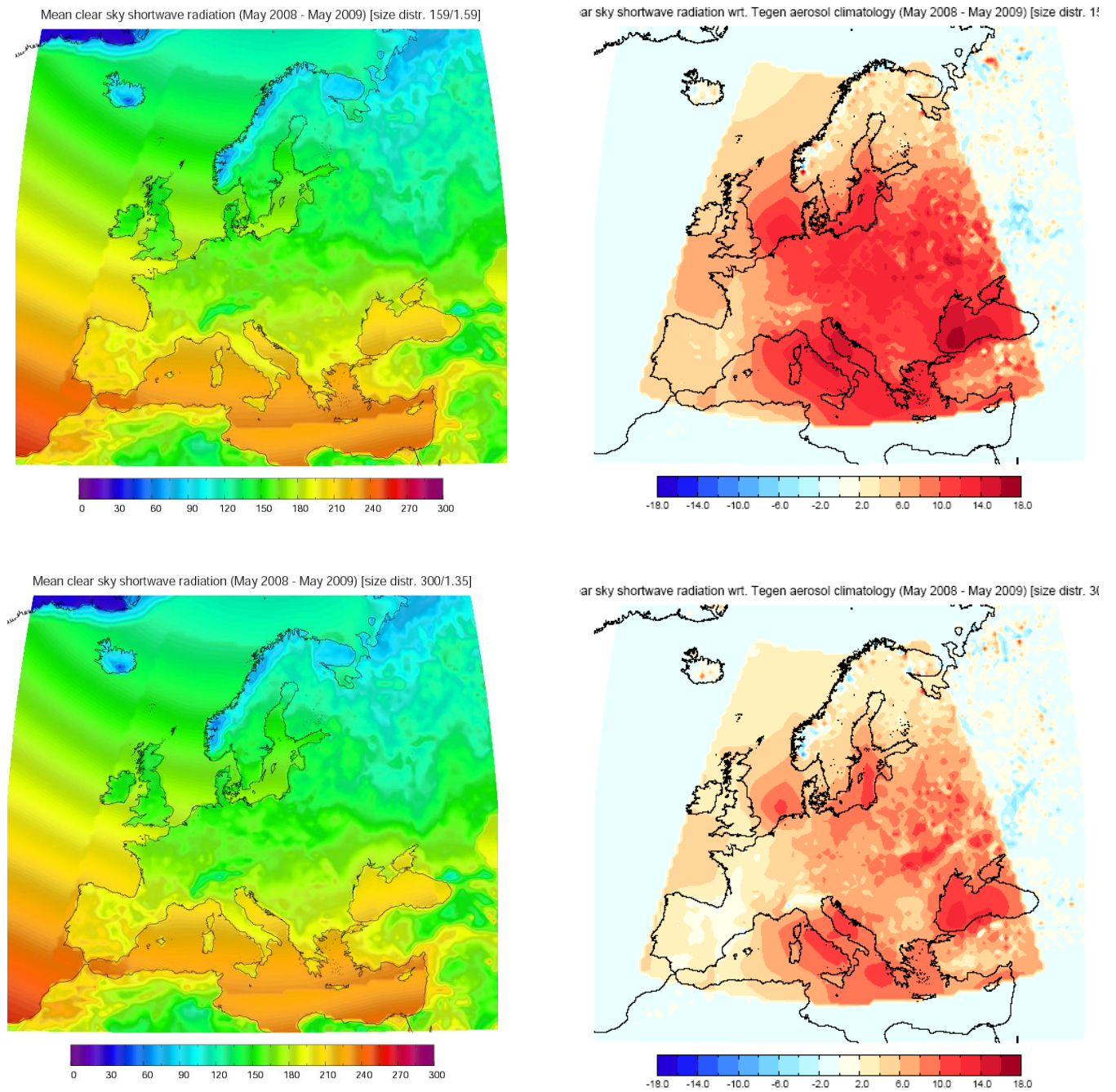


Figure 8 The impact of a reduction in AOD in the LOTOS-EUROS domain to the amount of clear sky incoming shortwave radiation at the surface. Panels on the left side show the absolute amount for the LE_159 (top panel) and LE_300 (bottom panel) experiment. Panels on the right side show the difference w.r.t. the reference experiment

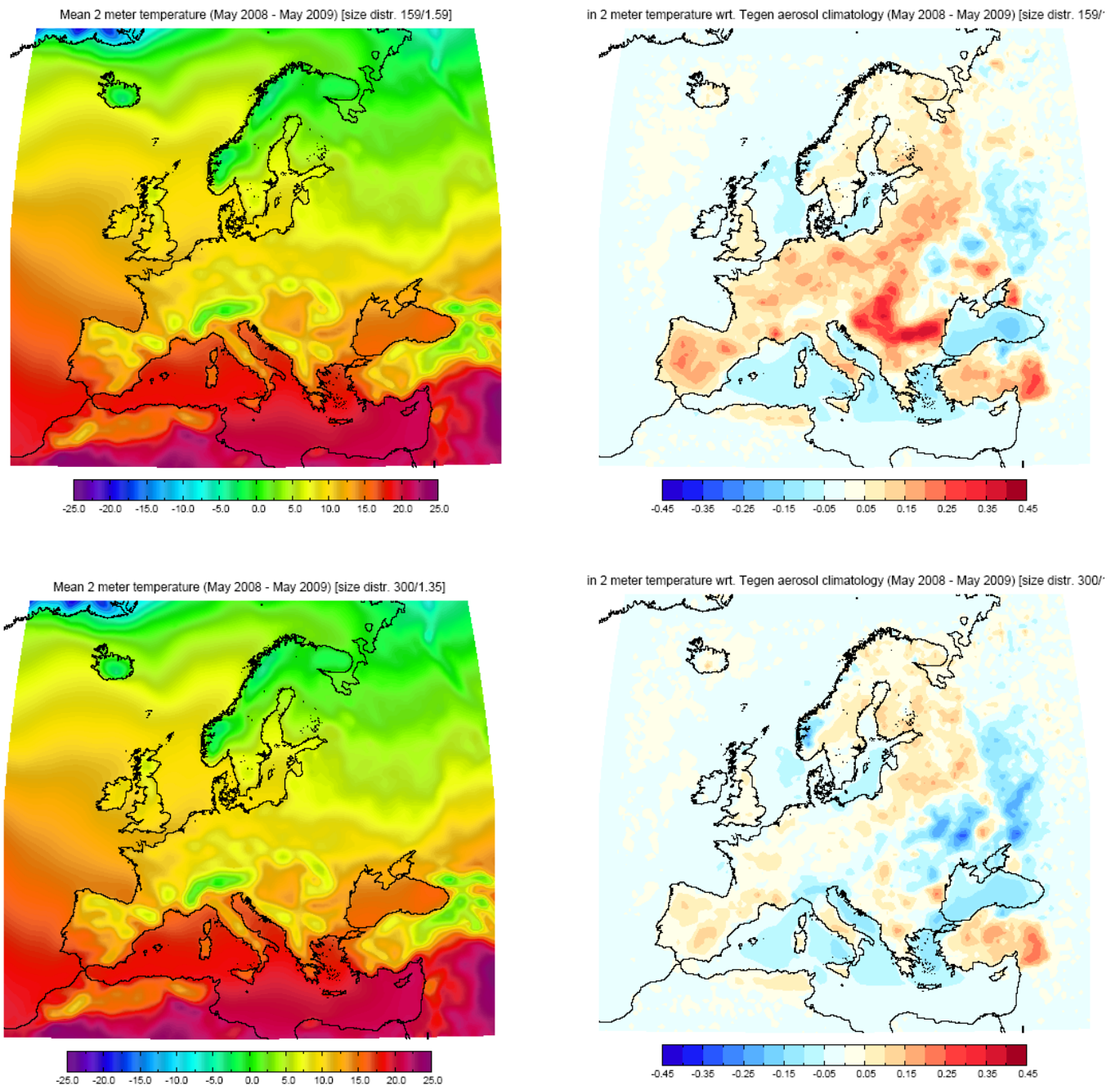


Figure 9 Like Figure 8 but for 2-meter temperature

The Figures 8 and 9 show the impact of differences in AOD on the clear-sky incoming short wave radiation at the surface and the 2-meter temperature, respectively. The reduction in AOD in going from the Tegen climatology to the LOTOS-EUROS forced AOD yields a discernable increase in clear-sky incoming short wave radiation at the surface, which on an annual basis amounts to 5-15 Wm² across the European continent. The effect on 2-meter temperature is somewhat more diverse because unlike AOD and the clear-sky short wave radiation clouds play an important role in determining the 2-meter temperature. Still, the LE_159 experiment yields a positive impact on 2-meter temperature for nearly the entire European land mass with differences up to 0.4 K over southern Rumania. However, there also some areas (e.g. the Ukraine) showing a decrease in temperature which is related to an increase in cloud amount which in these regions more than counteracts the effect of a reduced AOD. Over sea, the effect on temperature is very small to negligible, which is due to the fact that sea surface temperature is an externally prescribe parameter leaving little room for variations in the 2-meter temperature between the different experiments. The fact that the difference is slightly negative stems from the fact that a reduction in AOD corresponds to a reduction in atmospheric absorption of short wave radiation which results in a slightly colder atmosphere. This effect is as expected most prominent in predominately cloud free regions like e.g. the Mediterranean and the southern portion of the Black Sea. We also like to point out that in a coupled atmosphere-ocean model – like EC-Earth – a reduction in AOD over the oceans implies a significant source of extra heating of a shallow water layer just below the sea surface keeping in mind that the surface albedo of open water is very small.

4.2 Comparison to AERONET observations

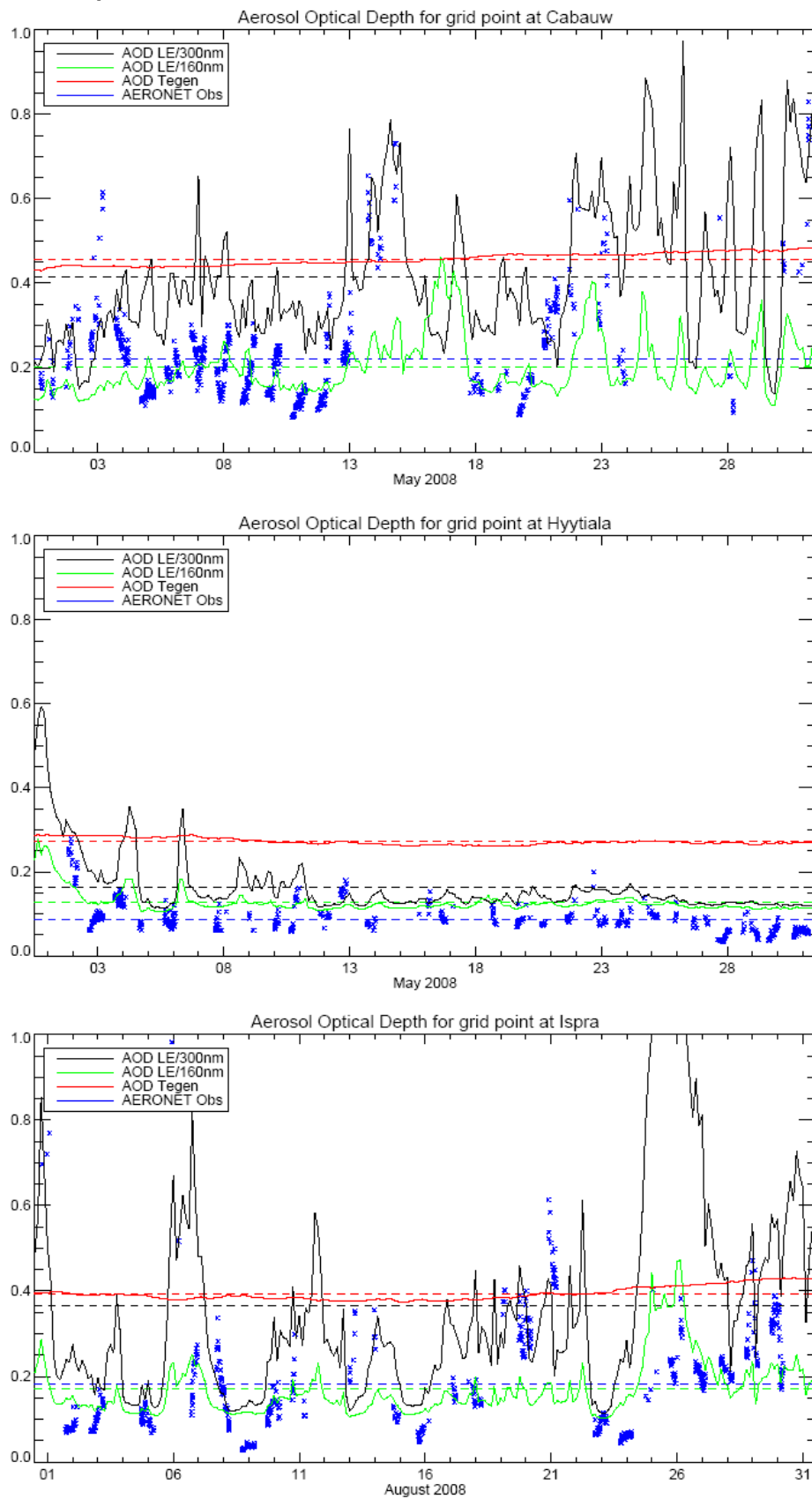


Figure 10 Observed and simulated AOD at Cabauw and Hyttiala for May 2008, and at Ispra for August 2008

Results from the three experiments have also been compared with ground-based observations conducted at three European sites, i.e. Cabauw, the Netherlands; Hyttiala, Finland; and Ispra, Italy. Figure 10 shows the time series of AOD observed at Cabauw and Hyttiala (May 2008) and at Ispra (August 2008) together with the simulated time series produced by the three experiments. The observed time series nicely show that there can be huge variations in AOD on a day-to-day or even sub-daily scale, in particular in Cabauw and Ispra, which are likely related to boundary-layer processes and/or variations in weather regime. The Figure also shows that the LOTOS-EUROS produced AOD time series are to some extent capable of capturing these variations, although often not with the correct magnitude or with the proper timing. Moreover, the LE_159 AOD estimates are comparing reasonably well on average with the observed value. Although initially the LE_300 AOD estimates seemed appropriate from the annual mean, they are surely too high on average, comparable in size with the Tegen values. However, on longer time scales the LE_159 AOD is found to underestimate the observed mean at Cabauw (shown in Figure 11) more substantially by about 30%, while it is better in line with the observations at Hyttiala and Ispra (not shown).

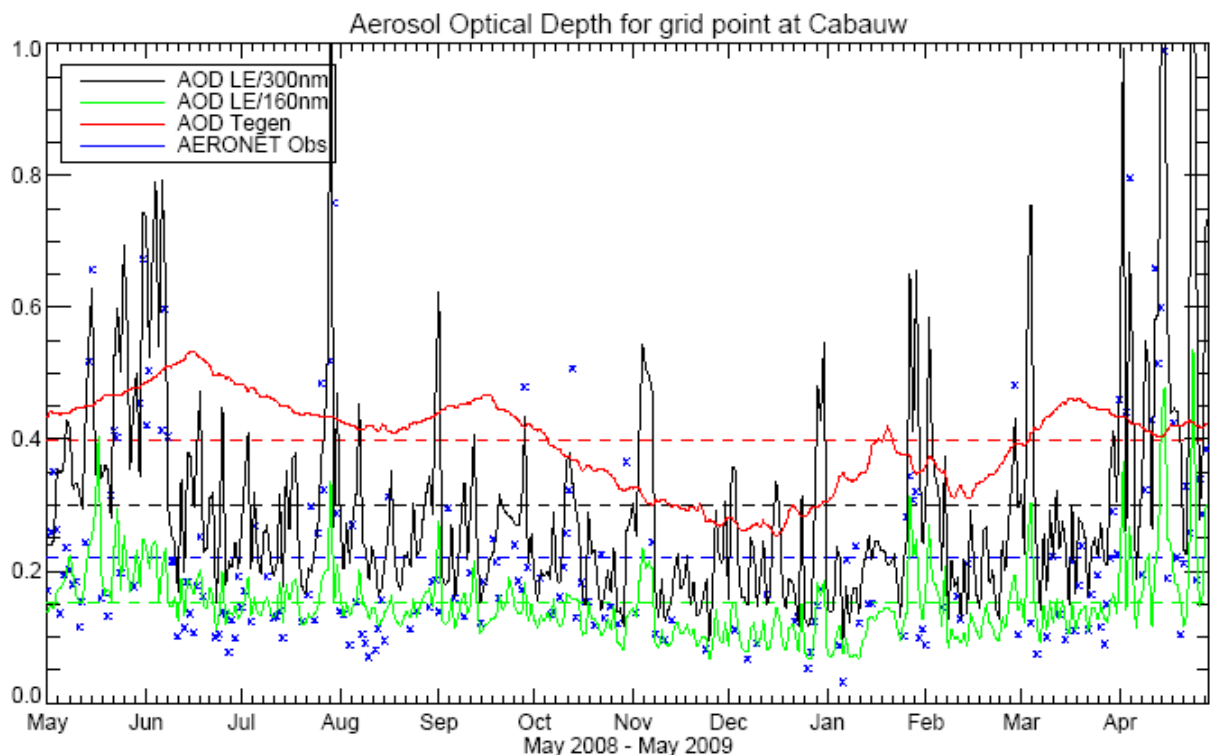


Figure 11 Observed and simulated AOD at Cabauw for the period May 2008 – May 2009

A point of concern is that in all cases there are many observations below the lowest values of modeled AOD. In the near future we will investigate this feature which we think is related to a currently inadequate assumption for the amount of aerosol loading in the atmosphere above the LOTOS-EUROS upper boundary positioned at 5km altitude.

Finally, Figure 12 shows a comparison of daily averaged simulated clear-sky incoming short wave radiation with observations at Cabauw. The observations are restricted to cloud free days. An attempt has also been made to develop a clear and clean sky estimate of the radiation at Cabauw which may be considered the theoretical upper limit. With this estimate, and the use of the measured AOD's at Cabauw, a synthesized value of the shortwave radiation is calculated. Regarding the two LE-experiments the clear sky short wave radiative fluxes corresponding to both experiments are mostly close together, with the LE_159 value always larger, but in June 2008 there were several days when the difference did grow above 20 Wm^{-2} . The radiation corresponding to Tegen is always the lowest among the simulated estimates with the exception of a few days with significant aerosol loading.

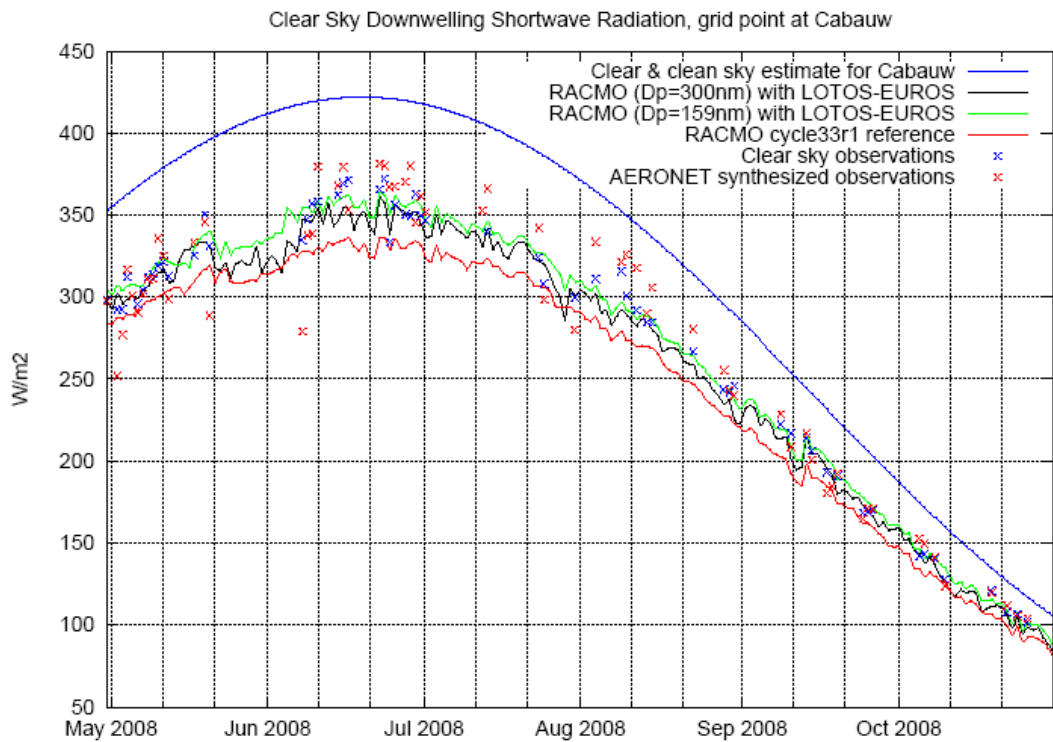


Figure 12 Daily mean clear sky incoming radiation at the surface at Cabauw for the period May 2008-October 2008. Observed values are restricted to cloud free days. Simulated curves are inferred from each of the three experiment. The blue curve represents a theoretical curve assuming a vertical atmospheric cloud free column with very dry and pristine conditions

5 Discussion

First of all, the project has resulted in a working system including the first direct aerosol effect. But further validation on more stations is required before the system can be used for climate-air quality interaction scenarios. Also the Tegen climatology could be replaced by CMIP5 to have a better reference for the validation.

LOTOS-EUROS tends to underestimate aerosol concentrations. For the operational forecasting a bias correction is used, which was not used in the present coupled version. This will lead to an underestimation of the aerosol effect. In newer versions of LOTOS-EUROS, this has partly been improved, by adding mineral dust emissions and changes in the deposition velocities. For reasons of consistency, the same version was used as for the one-way coupled runs. Also a good parameterization of secondary aerosols would improve the model, in particular in summer. Another improvement is the extension of LOTOS-EUROS with the aerosol module M7, which explicitly includes aerosol growth due to condensation and coagulation and allows for internally mixed particles (Manders and Schaap 2011). In the present coupled version, a fixed size distribution was assumed, this would not be necessary then. In addition, a vertical extension of the LOTOS-EUROS domain would improve the representation of aerosol above 5 km, which still has to be taken from climatology now.

While much progress has been made with the explicit treatment of the direct aerosol effect and the *first* aerosol indirect effect in the framework of the coupled RACMO-LOTOS-EUROS, an explicit treatment of the *second* aerosol indirect effect, i.e. the effect of aerosol on precipitation and cloud life time, is still lacking. A first step to include the second AIE has recently been made by the implementation and testing of a new microphysics parameterization scheme in the shallow convection module of the single column model (SCM) version of RACMO (Holtslag, 2011). In the new scheme the autoconversion process explicitly depends on CCN concentration scheme with the most rapid conversion occurring for low values in CCN ($< 200 \text{ cm}^{-3}$) and virtually no conversion for much higher ($> 500 \text{ cm}^{-3}$) values in CCN concentration unless the vertical cloud extent is large. In the context of the SCM, CCN concentration were prescribed and it was assumed that cloud droplet concentration (N_c) and CCN concentration are equal. Results from SCM simulations have been compared with observed precipitation, but the evaluated sample was limited nor was there a comparison with other quantities like cloud parameters.

It remains to be done to port the new microphysics scheme to RACMO 3D. The behaviour of the scheme in the – much less controlled - 3D context has to be analyzed, in particular the sensitivity to prescribed CCN concentration and to the parameters of the autoconversion scheme. It is probably also needed to generalize the microphysics scheme to other cloud parameterizations of RACMO (stratiform clouds, deep convective clouds). Next, the CCNs must be linked with the time-varying aerosol fields imported from LOTOS-EUROS in very much the same way as was done in setting up the explicit treatment of the first indirect effect. In essence, all tools and ingredients for carrying out the final step are already available. Once these steps have been completed, we have at our disposal a two-way coupled atmosphere-chemistry-transport model system offering us a powerful tool to investigate the impact of the three most relevant aerosol effects on the climate

system for present-day climate conditions as well as future climate conditions and/or scenarios.

Both RACMO2 and LOTOS-EUROS are under permanent development, when substantial improvements are made, new versions of the models can be coupled using the existing structures.

6 References

- Asmi, A. et al., (2011). Number size distributions and seasonality of submicron particles in Europe 2008-2009. *Atmospheric Chemistry and Physics Discussions*, Volume 11, Issue 3pp.8893-8976
- Christensen, J.H., and Christensen, O.B., (2007). A summary of the PRUDENCE model projections of changes in European climate by the end of this century. *Climate Change*, 81, 7-30.
- De Ruyter de Wildt, M., Eskes, H., Manders, A., Sauter, F., Schaap, M., Swart, D., van Velthoven, P., (2011). Six-day PM 10 air quality forecasts for the Netherlands with the chemistry transport model Lotos-Euros, *Atmospheric Environment* 45 (31) , pp. 5586-5594.
- De Martino, G., Bert van Uft, Harry ten Brink, Martijn Schaap, Erik van Meijgaard and Reinout Boers (2008). An aerosol-cloud module for inclusion in the KNMI regional climate model RACMO2. KNMI Scientific report WR 2008-05.
- EPA, National Ambient Air Quality Standards, <http://www.epa.gov/ttn/naaqs/>
- EU Directive 2008/50/EC of the European Parliament and of the Council of 21 May 2008 on ambient air quality and cleaner air for Europe, 2008.
- Hess, M., P. Koepke, and I. Schult, (1998). I. Optical Properties of Aerosols and Clouds: The Software Package OPCA, *B. Am. Meteorol. Soc.* **79**, 831-844,doi:10.1175/1520-0477.
- Holtslag, M.C., (2011) . Impact of aerosol on boundary-layer clouds and precipitation: small particles, large impacts. KNMI, Internship Report.
- Kinne, S., and Co-Authors, (2003). Monthly averages of aerosol properties: A global comparison among models, satellite data, and AERONET ground data, *J. Geophys. Res.*, **108**(D20), 4634, doi:10.1029/2001JD001253.
- Kuenen., J., H. Denier van der Gon, A. Visschedijk, H. van der Brugh and R. van Gijlswijk, (2011). MACC European emission inventory for the years 2003-2007. TNO report, UT-2011-00588.
- Lenderink, G, Van den Hurk, B., Van Meijgaard, E., Van Ulden, A.P. and Cuijpers, J.,(2003). Simulation of present-day climate in RACMO2: first results and model developments. KNMI technical report TR 252.
- Manders, A.M.M., Schaap, M., and Hoogerbrugge, R.,(2009). Testing the capability of the chemistry transport model LOTOS-EUROS to forecast PM10 levels in the Netherlands, *Atmospheric Environment*, 43 (26), pp. 4050-4059.
- Manders, A.M.M, van Uft, B., van Meijgaard, E., and Schaap, M., (2011). Coupling of the air quality model LOTOS-EUROS to the climate model RACMO, Dutch National Research Programme Knowledge for Climate Technical Report KFC/038E/2011, ISBN 978-94-90070-00-7.

Manders, A.M.M., Meijgaard, E. van, Mues, A.C., Kranenburg, R., Ulft, L.H. van, Schaap, M., (2012). The impact of differences in large-scale circulation output from climate models on the regional modelling of ozone and PM. Subm, to Atmos. Chem. Phys.

Martin, G.M., D.W. Johnson and A. Spice, (1994). The measurement and parameterization of effective radius of droplets in warm stratocumulus clouds, J. Atmos. Sci., 51, 1823-1842.

Mlawer, E.J. and Clough, S.A.,(1997). Shortwave and longwave enhancements in the rapid radiative transfer model. In Proc. 7th Atmospheric Radiation Measurement (ARM) Science Team Meeting, U.S. Department of Energy, CONF-9603149, available from http://www.arm.gov/publications/proceedings/conf07/extended_abs/mlawer_ej.pdf?id=10.

Meijgaard, E. van, Van Ulft, L.H., Van de Berg, W.J., Bosveld, F.C., Van den Hurk, B.J.J.M, Lenderink, G., Siebesma, A.P., (2008). The KNMI regional atmospheric climate model RACMO version 2.1. KNMI Technical report, TR-302 .

Meijgaard, E. van, L.H van Ulft, G. Lenderink, S.R. de Roode, L. Wipfler, R. Boers and R.M.A. Timmermans, (2011). Refinement and application of a regional atmospheric model for climate scenario calculations of Western Europe, CCsP Final report, KvR 054/12.

Menon, S., A. D. Del Genio, D. Koch and G. Tselioudis, (2002). GCM Simulations of the Aerosol Indirect Effect: Sensitivity to Cloud Parameterization and Aerosol Burden, J. Atmos. Sci., **59**, 692-713.

Mues, A., Manders, A., Schaap, M., Kerschbaumer, A., Stern, R., Bultjes, P., (2012). Impact of the extreme meteorological conditions during the summer 2003 in Europe on particulate matter concentrations. Atmospheric Environment, in press.

Petters, M. D. and S. M. Kreidenweis (2007). A single parameter representation of hygroscopic growth and cloud condensation nucleus activity, *AtmosChemPhys*, 7, 1961-1971.

Raes, F., Liao, H., Chen, W.-T. and Seinfeld, J.H., (2010). Atmospheric chemistry-climate feedbacks, Journal of Geophysical Research D, DOI: 10.1029/2009JD013300.

Savenije, M., Ulft, B, van, Manders, A, Meijgaard, E. van, (2012). Improvement and extension of the coupling between RACMO2 and LOTOS-EUROS. TNO report TNO-060-UT-2012-00496.

Schaap, M., R. M. A. Timmermans, F. J. Sauter, M. Roemer, G. J. M. Velders, G. A. C Boersen, J. P. Beck, and P. J. H. Bultjes, (2008). The LOTOS-EUROS model: description, validation and latest developments. Int. J. of Environ. and Pollution, 32, No. 2, pp.270–290.

Segelstein, D.J., (1981). The complex refractive index of water., Master's thesis, University of Missouri-Kansas City, USA.

Seinfeld, J.H. and Pandis, S., (2006). Atmospheric chemistry and physics. Wiley
Tai, A.P.K., Mickely, L.R., Jacob., D.J., (2010). Correlations between fine particulate matter (PM_{2.5}) and meteorological variables in the United States: implications for the sensitivity of PM_{2.5} to climate change. *Atmos. Env.* 44, 3976-3984, doi:10.1016/j.atmosenv.2010.06.060.

Tanré, D., J.-F. Geleyn, and J. Slingo, (1984). First results of the introduction of an advanced aerosol-radiation interaction in the ECMWF low resolution global model, in *Aerosols and Their Climatic Effects*, edited by H. Gerber and A. Deepak, pp. 133– 177, A. Deepak, Hampton, Va.

Tegen, I., P. Hoorig, M. Chin, I. Fung, D. Jacob, and J. Penner (1997), Contribution of different aerosol species to the global aerosol extinction optical thickness: Estimates from model results, *J. Geophys. Res.*, 102, 23,895– 23,915.

Zhang, Y., Wen, X.-Y., Jang, C.J., (2010). Simulating chemistry-aerosol-cloud-radiation-climate feedbacks over the continental U.S. using the online-coupled Weather Research Forecasting Model with chemistry (WRF/Chem), *Atmos. Env.* 44, 3568-3582.

7 Signature

Name and address of the principal

NMDC

Mr. J. Matthijssen

P.O. Box 201

3730 AE De Bilt

Names of the co-operators

Drs. M. (Mark) Savenije, KNMI

Dr. L.H. (Bert) van Uift, KNMI

Dr. E. (Erik) van Meijgaard, KNMI

Dr. J.S. (Bas) Henzing, TNO

J.M.J. (Joost) Aan de Brugh MSc, TNO

Dr. A.M.M. (Astrid) Manders-Groot, TNO

Dr. M. (Martijn) Schaap TNO

Date upon which, or period in which the research took place

Name and signature reviewer:



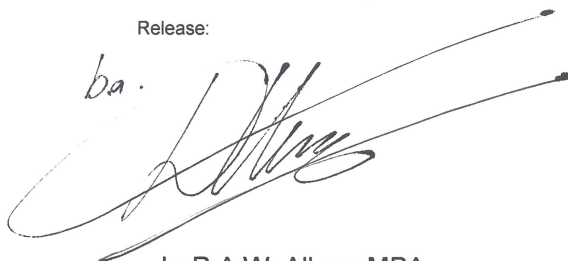
Dr. R.L. (Lyana) Curier, TNO

Signature:



Dr. A.M.M. Manders-Groot
Project leader

Release:



Ir. R.A.W. Albers MPA
Research Manager